Azoospermia in mice with targeted disruption of the *Brek/Lmtk2* (brain-enriched kinase/lemur tyrosine kinase 2) gene

Seiji Kawa*, Chizuru Ito†, Yoshiro Toyama†, Mamiko Maekawa†, Tohru Tezuka*, Takahisa Nakamura*, Takanobu Nakazawa*, Kazumasa Yokoyama*, Nobuaki Yoshida‡, Kiyotaka Toshimori†, and Tadashi Yamamoto*§

*Division of Oncology, and ‡Laboratory of Gene Expression and Regulation, Center for Experimental Medicine, Institute of Medical Science, University of Tokyo, Tokyo 108-8639, Japan; and †Department of Anatomy and Developmental Biology, Graduate School of Medicine, Chiba University, Chiba 260-8670, Japan

Edited by Ryuzo Yanagimachi, University of Hawaii, Honolulu, HI, and approved October 13, 2006 (received for review May 5, 2006)

Brek/Lmtk2 (brain-enriched kinase/lemur tyrosine kinase 2) is a member of the Aatyk family of kinases that comprises Aatyk1, Brek/Lmtk2/Aatyk2, and Aatyk3. Although several potential roles have been proposed for Brek and other Aatyk family members, the physiological functions of these kinases remain unclear. Here, we report that *Brek*$^{-/-}$ male mice are infertile, with azoospermia. Detailed histological analysis revealed that *Brek*$^{-/-}$ germ cells differentiated normally until the round-spermatid stage, but failed to undergo the normal change in morphology to become elongated spermatids. Testicular somatic cells appeared normal in these mice. Expression of Brek in testis was restricted to the germ cells, suggesting that the maturations of germ cells in *Brek*$^{-/-}$ mice are affected in a cell-autonomous manner. On the basis of these findings, we concluded that Brek is essential for a late stage of spermatogenesis. Further clarification of the mechanism by which Brek regulates spermatogenesis may help identify new targets for reproductive contraceptives and treatments against infertility.

AATYK | BREK | infertility | LMTK2 | spermatogenesis

Spermatogenesis, the process by which primordial germ cells generate sperm, is a complex process that includes mitotic division of spermatogonia, meiotic division of spermatocytes to generate haploid cells called spermatids, and differentiation of the spermatids into sperm cells. The last maturation step in which haploid spermatids undergo a complex restructuring program is called spermiogenesis. Spermiogenesis begins with formation of the acrosome from Golgi-derived vesicles, followed by formation of a flagellum, condensation of the nucleus with DNA compaction, and jettison of the cytoplasm. The resulting mature sperm consists of a head with a nucleus and a tail and enters the lumen of the seminiferous tubules. Spermatozoa that differentiate in the testis mature further during the passage through the epididymal duct to acquire functions essential for fertilization.

Protein-phosphorylation events play pivotal roles in regulating intracellular signals in response to a wide variety of stimuli. There is accumulating evidence that protein kinases, such as c-Kit, play critical and distinct roles in spermatogenesis (1). Brek (brain-enriched kinase) is a member of the protein kinase subfamily that comprises Aatyk1, Brek/Lmtk2/Aatyk2, and Aatyk3. This kinase subfamily was recently identified through a genome database search for human tyrosine kinases and was tentatively named the Aatyk (apoptosis-associated tyrosine kinase) subfamily (2). Generation of a phyletic tree of known tyrosine and Ser/Thr kinases revealed that Aatyk family kinases represent a previously uncharacterized category of kinases that reside between tyrosine kinases and Ser/Thr kinases. The primary structures of Aatyk kinases show slightly higher homology to tyrosine kinases than to Ser/Thr kinases, but we previously showed that the Aatyk kinases are Ser/Thr kinases and not tyrosine kinases (3). Although Brek is also called Aatyk2 and Lmtk2 (lemur tyrosine kinase 2), these names are apparently after the putative tyrosine kinase activity and do not accurately reflect its genuine property. We also showed that Brek is expressed at high levels in early postnatal brain and that Brek plays a part in nerve growth factor (NGF) signaling in PC12 cells (3). Other groups reported that Kpi-2 (kinase/phosphatase/inhibitor-2) and Cprk (CDK5/p35-regulated kinase), which are identical to Brek, interact with protein phosphatase 1 catalytic subunit (PP1C) and p35 *in vitro* (4, 5); however, their *in vivo* association and biological significance are not characterized.

In this study, we elucidated the physiological function of Brek by generating mice with a targeted disruption of the *Brek* gene. We found that *Brek*$^{-/-}$ male mice are infertile, with azoospermia. Because mice lacking members of the Aatyk family have not been analyzed, our current study provides a clue to investigate the physiological roles of this unique and little characterized family of kinases and to the molecular mechanism of spermatogenesis.

Results

Generation of *Brek*-Knockout Mice. To investigate the physiological role of mammalian Brek, we generated mice with targeted disruption of *Brek*. A *Brek*-targeting construct was designed to replace the genomic region of *Brek* containing exons 4–6 with a neomycin-resistance cassette (Neo) (Fig. 6*A*, which is published as supporting information on the PNAS web site). The exons 4–6 encode amino acid residues essential for kinase activity. ES cell clones bearing the targeted allele were selected by Southern blot analysis (Fig. 6*B*). To generate homozygous mutant mice, F_1 heterozygotes were interbred, and the F_2 offspring were genotyped by PCR analysis (Fig. 6*C*). Absence of Brek protein in *Brek*$^{-/-}$ mice was confirmed by immunoblot analysis of brain lysates (Fig. 6*D*).

Azoospermia in *Brek*-Knockout Mice. *Brek*$^{-/-}$ mice were born at a slightly lower frequency (18%, $n = 268$) than the predicted Mendelian frequency. We have not yet examined when and how the missing 7% of *Brek*$^{-/-}$ pups die before birth. Null pups that survived the gestation period showed no phenotypic abnormality at birth and had apparently normal growth. Histological examination of immature *Brek*$^{-/-}$ mice (postnatal weeks 3 and 4)

Author contributions: S.K., T. Nakamura, T. Nakazawa, K.T., and T.Y. designed research; S.K., C.I., Y.T., and M.M. performed research; S.K., K.Y., and N.Y. contributed new reagents/analytic tools; S.K., C.I., Y.T., M.M., and K.T. analyzed data; and S.K., T.T., T. Nakamura, K.Y., K.T., and T.Y. wrote the paper.

The authors declare no conflict of interest.

This article is a PNAS direct submission.

Abbreviation: PP1C, protein phosphatase 1 catalytic subunit.

§To whom correspondence should be addressed at: Division of Oncology, Institute of Medical Science, University of Tokyo, Shirokanedai 4-6-1, Minato-ku, Tokyo 108-8639, Japan. E-mail: tyamamot@ims.u-tokyo.ac.jp.

www.pnas.org/cgi/doi/10.1073/pnas.0603603103

Table 1. Fertility assessment

Male	Female	Average number of litters
$Brek^{+/-}$	$Brek^{-/-}$	6.1 ± 3.8 (n = 4 plugs)
$Brek^{+/-}$	$Brek^{+/-}$	7.2 ± 1.4 (n = 10 plugs)
$Brek^{-/-}$	$Brek^{+/-}$	0 (n = 6 plugs)

showed that all tissues examined, including testis (both somatic and germ cells), epididymides, and prostate were normal (data not shown). Note that spermatozoa are not typically present during this period. Adult $Brek^{-/-}$ mice were healthy, with normal size and behavior. However, in breeding experiments, male $Brek^{-/-}$ mice were infertile, although male $Brek^{+/-}$ and female $Brek^{-/-}$ mice showed normal fertility (Table 1). To determine the cause of infertility in the $Brek^{-/-}$ males, we first examined whether spermatozoa were produced normally at 8 weeks of age. Testes of $Brek^{-/-}$ mice were smaller than those of $Brek^{+/+}$ mice (Fig. 1*A*). There were no spermatozoa in the epididymides of $Brek^{-/-}$ mice (Fig. 1*B*). Thus, infertility of $Brek^{-/-}$ males appeared to be caused by impaired spermatogenesis. Testes weights and sperm counts of $Brek^{+/-}$ mice were normal (data not shown). Because testicular size and germ cell morphology during immature periods appeared normal, the defects in $Brek^{-/-}$ mice seemed to be in late spermatogenesis. By TUNEL assay against sections of adult seminiferous tubules, we found a markedly increased number of apoptotic cells in $Brek^{-/-}$ testes (Fig. 2). This finding suggested that differentiation of $Brek^{-/-}$ germ cells was perturbed during late spermatogenesis and that a subset of the perturbed germ cells in $Brek^{-/-}$ testes underwent apoptosis.

Importance of Brek in Late Spermatogenesis. To clarify defects in spermatogenesis in $Brek^{-/-}$ mice, we performed histological analyses of adult seminiferous tubules in detail (Fig. 3). Although spermatogenesis proceeded normally in $Brek^{-/-}$ testes until approximately round-spermatid production, $Brek^{-/-}$ spermatids showed abnormalities in further development (Fig. 3 *B*, *D–I*, and *K*). The number of elongating spermatids was gradually reduced in $Brek^{-/-}$ testes as spermiogenesis proceeded. Few elongated spermatid were observed in seminiferous epithelium of $Brek^{-/-}$ testes at stages VII–VIII (Fig. 3 *B*, *D*, *E*, and *K*), unlike

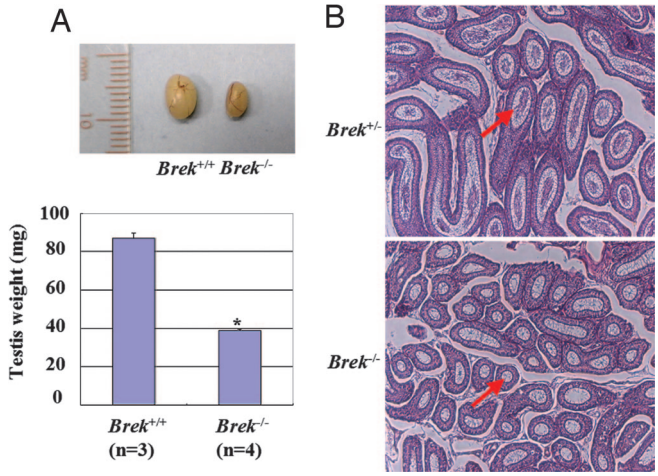

Fig. 1. Azoospermia in $Brek^{-/-}$ mice. (*A*) Comparison of testis weights of 8-week-old $Brek^{+/+}$ and $Brek^{-/-}$ mice. (*Upper*) Photographs of testes from $Brek^{+/+}$ and $Brek^{-/-}$ mice. (*Lower*) One testis from each pair of testes was trimmed free of fat and weighed. (*B*) Sperms in epididymis. Micrographs of H&E-stained sections from 8-week-old $Brek^{+/-}$ and $Brek^{-/-}$ epididymides. Arrows indicate presence ($Brek^{+/-}$) or absence ($Brek^{-/-}$) of sperm cells. Analysis with 12-week-old mice yielded comparable results.

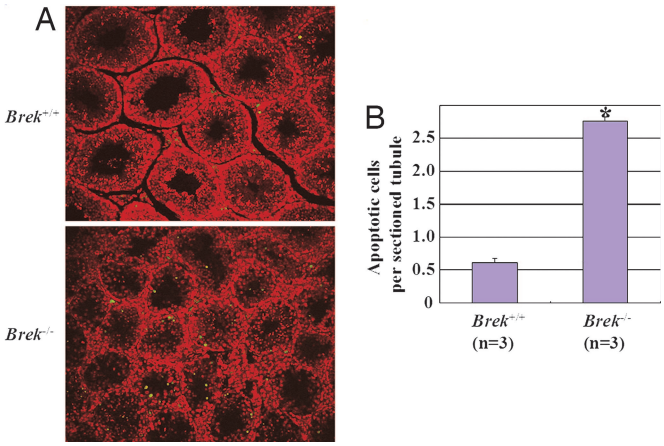

Fig. 2. Increased germ cell apoptosis in $Brek^{-/-}$ mice. (*A*) Apoptotic cells were detected by *in situ* TUNEL assay of testis sections from 8-week-old $Brek^{+/+}$ and $Brek^{-/-}$ mice. Cells were visualized with DAPI (red). Merged images show TUNEL-positive cells in yellow. (*B*) Quantification of apoptotic germ cells in the seminiferous tubules of 8-week-old $Brek^{+/+}$ and $Brek^{-/-}$ mice. In each testis, TUNEL-positive cells in at least 100 tubule sections were counted and averaged. Error bars represent SD. Statistical significance (*, $P < 0.01$) was assessed by Student's *t* test. Analysis of 12-week-old mice yielded similar results.

in that of $Brek^{+/+}$ testes (Fig. 3 *A*, *C*, and *J*). In addition, vacuoles and degenerated symplast-like cells were frequently found in $Brek^{-/-}$ seminiferous epithelium (Fig. 3 *B*, *E*, and H). Electron micrographs suggested that elongating spermatids were readily phagocytized by Sertoli cells in $Brek^{-/-}$ testes (Fig. 3 *E* and *H*). As a result, engulfed spermatids and residual bodies of spermatids were frequently observed in the cytoplasm of Sertoli cells near the basement membrane (Fig. 3*E*). Many of elongating spermatids in $Brek^{-/-}$ testes had variously deformed acrosomes. Typical acrosome deformation was indentation at the acrosome granule area (Fig. 3*F*). Many of $Brek^{-/-}$ spermatids that differentiated into elongated spermatid stage (step S14) were being degenerated and showed various deformations on the heads and tails (Fig. 3 *G* and *H*). Collapsed and separated acrosomes and tail degeneration with mitochondrial separation were often observed in $Brek^{-/-}$ testes (Fig. 3*H*). Flagellum development in late spermatids was not impaired in $Brek^{-/-}$ testes. The tail components such as outer dense fibers and fibrous sheath were apparently formed (Fig. 3*I*). We found few spermatids that differentiated to step S15 in seminiferous epithelium of $Brek^{-/-}$ testes (Fig. 7, which is published as supporting information on the PNAS web site). The number and morphology of testicular somatic cells, including Sertoli cells (Fig. 3 *A* and *B*) and Leydig cells (data not shown), in $Brek^{-/-}$ mice were indistinguishable from those in $Brek^{+/+}$ mice. Thus, the absence of Brek did not affect meiotic division of germ cells but abrogated the further maturation of round spermatids. Brek may control the activities of key proteins involved in late spermatogenesis.

Expression of Brek in Testis. Defects in testicular germ cells and somatic cells result in azoospermia. Abnormalities in hormone levels are also the cause of infertility. To characterize the expression profile of Brek in testis, we performed Western blot analysis (Fig. 4). Brek was highly expressed in mouse testis, suggesting that the impaired maturation of $Brek^{-/-}$ germ cells was due directly to defects in the testicular cells and not to indirect effects of defects in other cell types, such as neural cells (Fig. 4*A*). Consistently, serum levels of testosterone, luteinizing hormone, and follicle-stimulating hormone were not altered in $Brek^{-/-}$ male mice (Table 2). We further evaluated Brek expression in testes from C57BL/6 mice (postnatal weeks 2–10) and

DEVELOPMENTAL BIOLOGY

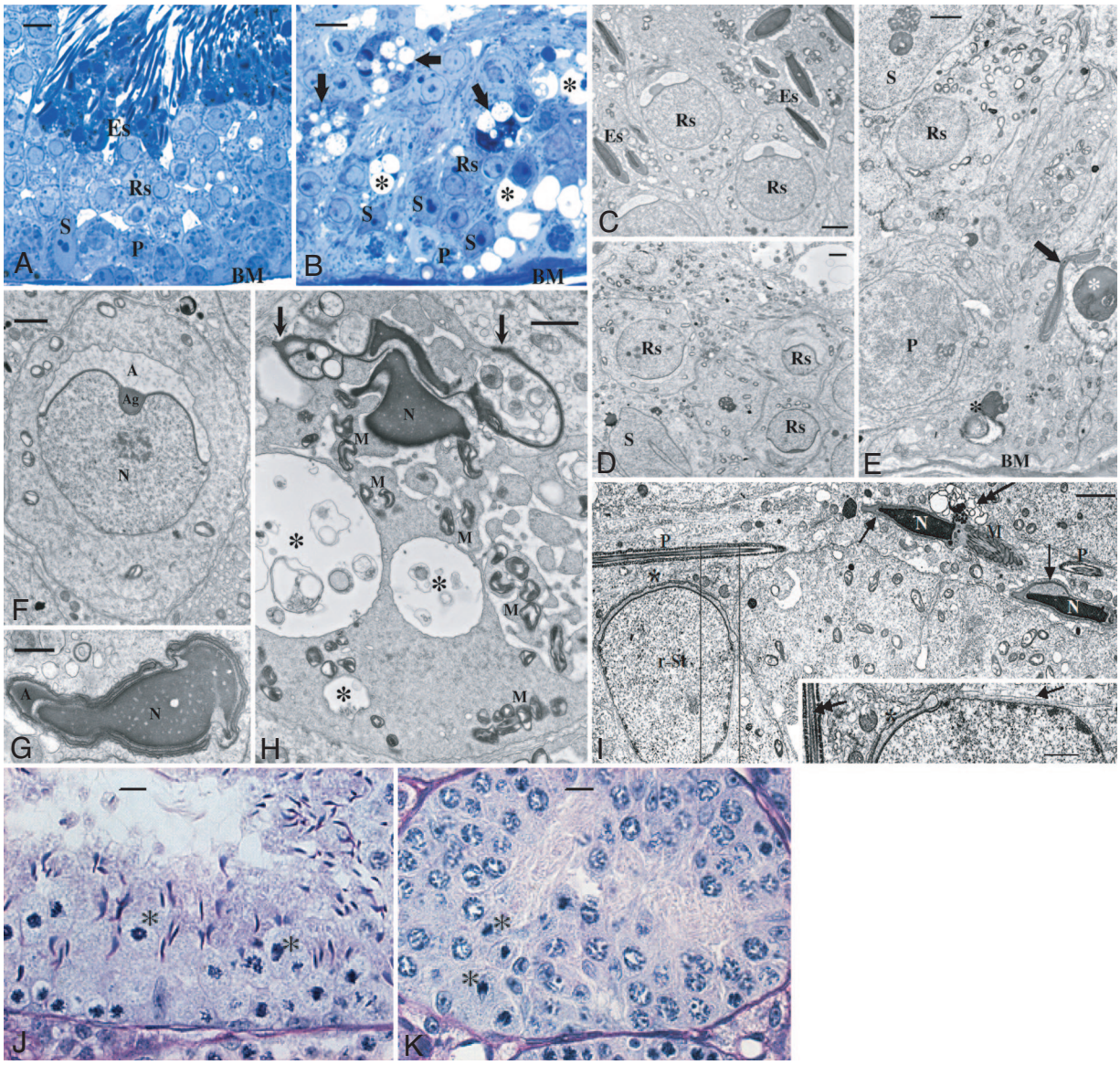

Fig. 3. Histological abnormality in *Brek*$^{-/-}$ testes. (*A* and *B*) Light micrographs of testes (around stage VII–VIII). Sections were stained with toluidine blue. (*A*) Normal spermatogenesis in *Brek*$^{+/+}$ testis. (*B*) Vacuoles (*) and degenerated symplast-like cells (arrows) were found in *Brek*$^{-/-}$ testis. (*C–I*) Electron micrographs of *Brek*$^{+/+}$ (*C*) and *Brek*$^{-/-}$ (*D–I*) testes. Sections were stained with lead and uranyl acetate. (*C*) Normal spermiogenesis with healthy round and elongating spermatids in *Brek*$^{+/+}$ testis. (*D*) In *Brek*$^{-/-}$ testis, round spermatids appear to be produced normally but gradually show abnormal development in the acrosome (*F*). (*E*) Elongating spermatids develop abnormally and are eventually engulfed by Sertoli cells (arrows) with residual bodies (*). (*G* and *H*) Elongated spermatids at step S13–14 in *Brek*$^{-/-}$ testes, showing varieties of deformations and collapsed components such as acrosome and nucleus in the head (*G*). Collapsed acrosomes (arrows) and vacuoles (*) found in Sertoli cells are indicated (*H*). (*I*) A few elongated spermatids survived until approximately step 15. Irregular acrosomes (arrows) and condensed nuclei (N) are indicated. The spermatids show electron-dense material with many vesicular structures at the border between the head and tail (double arrow). Middle piece shows relatively well arranged mitochondrial sheath (M) and principal piece region with fibrous sheath (P). A developed round spermatid (r-St) has an irregular acrosome (*), a part of which is shown in *Inset*. (*Inset*) A higher-magnification image of the rectangular area. Shown are manchette (arrow), irregular acrosome (*), and tail components such as fibrous sheath and outer dense fibers (double arrow; the axoneme is not clearly recognized at this magnification). (*J* and *K*) Stage matched images of *Brek*$^{+/+}$ (*J*) versus *Brek*$^{-/-}$ testes (*K*). Periodic acid/Schiff (PAS) staining shows stage XII that can be identified with secondary spermatocytes dividing at meiosis II (*). There are many elongating spermatids with PAS-positive acrosomes in the tubule of *Brek*$^{+/+}$ testis (*J*). Few or no elongating spermatids are survived in the tubule of *Brek*$^{-/-}$ testis (*K*). A, acrosome; Ag, acrosome granule; BM, basement membrane; Es, elongating or elongated spermatid; M, mitochondria; N, nucleus; P, pachytene spermatocyte; Rs, round spermatid; S, Sertoli cell. {Scale bar: 10 μm [*A* and *B*]; 2 μm [*C–E* and *I* (*Inset*, 1 μm)]; 1 μm [*F* and *H*]; 0.5 μm [*G*]; and 10 μm [J, K]}

kit mutant (*kit*$^{W/W-v}$) mice (postnatal week 10) (Fig. 4*B*). At postnatal week 10, the expression level of Brek was significantly low in *kit*$^{W/W-v}$ males compared with that in control wild-type males. Because *Kit*$^{W/W-v}$ males have greatly reduced numbers of germ cells but approximately normal number of somatic cells (6), the result suggested that Brek is expressed primarily in germ cells. Expression levels of Brek in testes of C57BL/6 mice were markedly increased between postnatal weeks 2 and 3 (Fig. 4*B*). This finding is consistent with our hypothesis that Brek is required for a late phase of spermatogenesis after meiosis, because the first wave of cells undergoing spermatogenesis reaches spermatid production stage during the periods analyzed (7). We further examined the expression of Brek using fractionated mouse testicular cells (i.e., the germ cells, Leydig cells, and

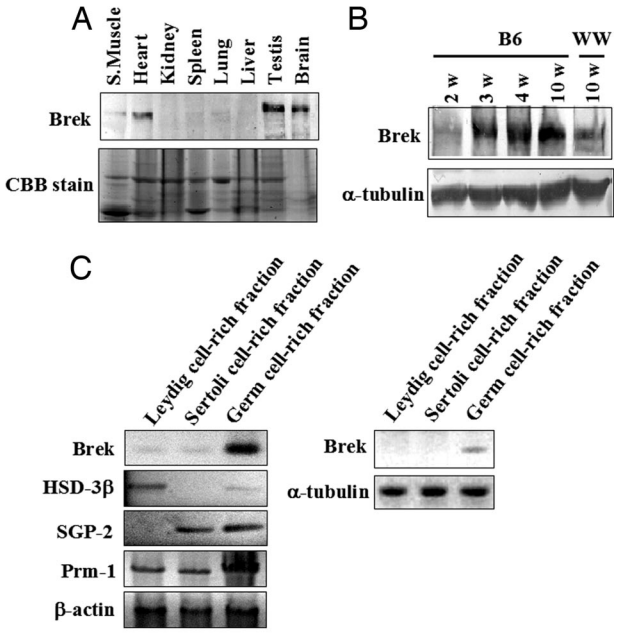

Fig. 4. Expression profile of Brek protein. (*A*) Mouse tissue lysates from 8-week-old males were probed with antibodies against Brek. Total protein levels were evaluated by Coomassie brilliant blue staining. (*B*) Testis lysates from *kit*$^{W/W-v}$ mice (WW; Postnatal week 10) and C57BL/6 mice (B6; Ages are indicated) were probed with antibodies against Brek. α-Tubulin was examined as a loading control. (*C*) Germ cell-, Sertoli cell-, and Leydig cell-rich fractions were prepared for RT-PCR analysis (*Left*) and Western blot analysis (*Right*) as described in *Materials and Methods*. The quality of fractionated cells was verified by RT-PCR of *3β-HSD*, *protamine-1*, and *SGP-2* genes, which are known to be specifically expressed in Leydig, germ, and Sertoli cells, respectively (*Left*). β-Actin and α-tubulin were examined as controls.

Sertoli cells) (Fig. 4*C*). Western blotting and RT-PCR using the fractionated cells revealed that *Brek* was exclusively expressed in a germ cell-rich fraction (Fig. 4*C*). Furthermore, immunohistochemical analysis of seminiferous tubules revealed that Brek was expressed at the elongating spermatid zone near the center of the seminiferous tubule. These findings are consistent with the phenotype in *Brek*$^{-/-}$ testes, in which germ cells failed to undergo the normal change in morphology to become elongated spermatids (Fig. 5). Therefore, we have concluded that impaired maturation of *Brek*$^{-/-}$ spermatids is a consequence of the cell-autonomous defects in *Brek*$^{-/-}$ germ cells.

Discussion

Our present study on *Brek*$^{-/-}$ mice revealed that Brek plays an essential role during spermatogenesis. Aatyk family kinases, including Brek, are evolutionarily distinct within the kinase subfamilies. The characteristics of Aatyk kinases in terms of amino acid sequences are intermediate between those of the tyrosine kinases and Ser/Thr kinases, which may explain why these kinases had escaped identification with classic homology-based screenings. *Aatyk1* was originally identified as a gene with expression up-regulated during apoptosis of myeloid cells (8). Aatyk1 is preferentially expressed in brain (9, 10), and several potential roles have been proposed in the nervous system, including regulation of neural differentiation (10) and apoptosis (11, 12). However, these potential roles were evaluated with *in vitro* experiments only, and definitive evidence for the role of Aatyk1 has not yet been reported. *Brek* and *Aatyk3* were originally identified in a human genome database as genes with kinase domain sequences that show high homology (≈50%) to that of *Aatyk1* (2). We previously reported that Brek is involved in NGF signaling in PC12 cells (3). In PC12 cells, Brek was phosphorylated rapidly upon stimulation with NGF in a TrkA- and protein kinase C-dependent pathway. Introduction of a kinase-defective mutant of Brek into PC12 cells enhanced both Erk phosphorylation and neurite outgrowth in response to NGF, suggesting that Brek is a negative regulator of NGF-induced neuronal differentiation. Other groups reported that Brek interacts with p35/Cdk5 (4) and Inhibitor-2/PP1 (5). However, the specific functions of Brek in physiological processes are not known, as is the case with Aatyk1. No functional or biochemical analyses of Aatyk3 have been reported. Thus, this study reports a previously uncharacterized physiological role of the Aatyk family members.

Table 2. Hormonal levels

	Teststerone, ng/dl	LH, ng/ml	FSH, ng/ml
Brek$^{+/+}$	24 ± 7 (n = 12)	4.1 ± 2.1 (n = 3)	93 ± 12 (n = 3)
Brek$^{-/-}$	31 ± 14 (n = 10)	3.3 ± 1.7 (n = 3)	85 ± 19 (n = 3)

LH, luteinizing hormone; FSH, follicle-stimulating hormone

Brek$^{-/-}$ mice had apparently normal health, with the exception of azoospermia. Despite the high expression of Brek in brain, no histological abnormalities in the nervous system have been yet found in *Brek*$^{-/-}$ mice. Because our previous results suggested that Brek is a negative regulator of NGF signaling in PC12 cells (3), we carried out histological analysis of the nervous system, especially forebrain cholinergic neurons and peripheral trigeminal neurons, whose development was significantly impaired in TrkA- or NGF-knockout mice (13, 14). However, no abnormality in the nervous system has been found in *Brek*$^{-/-}$ mice (data not shown). Because Aatyk1 and Aatyk3, as well as Brek, are expressed at high levels in brain (3), it is possible that Brek function in the nervous system is compensated for by other Aatyk family kinase(s) in *Brek*$^{-/-}$ mice. Therefore, generation of double- or triple-knockout mice that lack Aatyk1 and/or Aatyk3 in addition to Brek will further reveal physiological roles of Aatyk family kinases.

In this study, we found that male infertility in *Brek*$^{-/-}$ mice was due to impaired maturation of germ cells. We proposed that the impaired spermatogenesis in *Brek*$^{-/-}$ testis was directly caused by a defect in the germ cells and was not a secondary effect due to an abnormality in other cell types. In some strains of genetically modified mice, impaired spermatogenesis is a consequence of defects in testicular somatic cells (most frequently in Sertoli cells) or abnormalities in hormone levels (15–17). However, the number and morphology of testicular somatic cells were normal, and hormonal levels were not altered in *Brek*$^{-/-}$ mice. Importantly, testicular expression of Brek is restricted to germ cells, suggesting that the maturation of germ cells in *Brek*$^{-/-}$ mice is affected in a cell-autonomous manner.

Although differentiation of spermatogonia until step S1 (round spermatid) occurred normally in *Brek*$^{-/-}$ testes, further differentiation of spermatids was largely suppressed (Fig. 7). Accordingly, we found few spermatids that differentiated to step S15 in *Brek*$^{-/-}$ testes. Thus, Brek appears to be necessary for the morphological progression of postmeiotic germ cells, a process that includes mitochondrial compaction and expulsion of the cytoplasm, but not to be essential for the early phase of spermatogenesis. In wild-type mice, the first wave of spermatogenesis begins shortly after birth, and spermiogenesis is first observed around postnatal day 20 (7). The first spermatozoa are produced at approximately day 35. Our finding that the level of Brek protein in testis was increased between 2 and 3 weeks after birth was consistent with the idea that Brek expression is associated with a late phase of spermatogenesis, possibly after the generation of round spermatids. Importantly, immunohis-

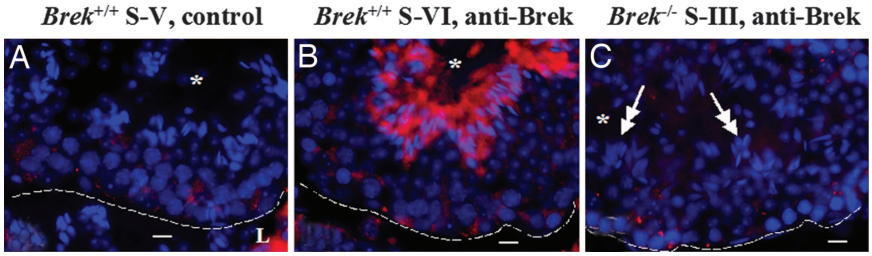

Fig. 5. Indirect immunofluorescence images of the seminiferous tubule. (*A*) Control image for $Brek^{+/+}$ testis at approximately stage V. Primary antibody (anti-Brek antibody) was omitted. Nonspecific staining (red) is found in the abluminal side of the tubule and in the interstitial Leydig cell (L). (*B*) Immunostaining with anti-Brek antibody for $Brek^{+/+}$ testis at approximately stage VI. Note strong staining (red) at the elongating spermatid zone near the center of the tubule. (*C*) Staining with anti-Brek antibody for $Brek^{-/-}$ testis at approximately stage III. No immunostaining in the region of developing spermatids (double arrows). Asterisk (*) shows the center of the tubule. Red, Alexa Fluor 546; blue, Hoechst 33258. Dotted line shows the basement membrane region, i.e., the border of the seminiferous tubule. (Scale bar: 10 μm.)

tochemical analysis revealed that Brek was expressed mainly in elongating and elongated spermatids in wild-type seminiferous tubules. We also found that mRNAs for genes expressed in postmeiotic germ cells, such as *Prm1*, *Prm2*, *TP1*, *TP2*, *CREM*, and *CaMK4* mRNAs, were also expressed in $Brek^{-/-}$ testis (data not shown), further supporting the hypothesis that $Brek^{-/-}$ germ cells differentiate normally into round spermatids. In addition, histological analysis of testes from immature $Brek^{-/-}$ mice (postnatal weeks 3 and 4) showed no abnormalities in the number and morphology of round spermatids (data not shown; note that the first wave of spermatogenesis has not reached the step of elongation of spermatids during this period).

The mechanism by which Brek contributes to the late phase of spermatogenesis is presently unknown. Brek was reported to bind to and phosphorylate the catalytic subunit of PP1 *in vitro* (5), suggesting that Brek may play a part in spermatogenesis through the regulation of PP1 activity. One of PP1 isoforms, PP1cγ2, is predominantly expressed in testis (18). Male mice with a targeted disruption of the *PP1cγ2* gene showed comparable phenotype with $Brek^{-/-}$ mice, severe impairment of spermiogenesis beginning at the round spermatid stage (18). It is possible that Brek regulates cytoskeletal structures needed for normal morphological development of round spermatids. Brek activity was rapidly increased upon lysophosphatidic acid (LPA) stimulation in PC12 cells, and overexpression of Brek promoted LPA-induced neurite retraction in differentiated PC12 cells (our unpublished data). Because LPA regulates actin cytoskeleton through RhoA, Brek might enhance the activity of RhoA. PP1 could also play a role in this scenario, because PP1 acts as a myosin phosphatase that is a key regulator of the actin cytoskeleton in skeletal muscle (19). In addition, NGF-PKC signaling might be also involved in the mechanism by which Brek play a role in spermatogenesis, such as in neurite elongation of PC12 cells. NGF and TrkA mRNAs were found principally in spermatocytes and round spermatids of the adult mouse testis, suggesting that NGF signaling might be involved in an early phase of spermiogenesis (20, 21). Multiple isozymes of PKC including α, β, δ, and ε isozymes are also expressed in testicular germ cells (22). In particular, like that of Brek, expression of PKC-δ in testis was increased between 2 and 3 weeks after birth (22). Further studies will define the precise mechanism by which Brek participates in spermatogenesis.

Fertility depends on the coordinated and combined functions of both the male and female reproductive systems. Anatomical defects, endocrinopathies, immunological problems, and environmental exposures are significant causes of infertility. Although several infertility disorders are associated with defined genetic syndromes, including cystic fibrosis and Turner syndrome (23, 24), nearly 25% of clinical infertility cases are idiopathic. Genetic etiologies are thought to underlie many of these unrecognized pathologies. Reproductive defects as a major phenotype in mutant mice such as the $Brek^{-/-}$ mice are being identified rapidly and may be helpful in refining our understanding of mechanisms underlying reproductive function, in identifying potential new contraceptive targets, and identifying the causative genes for specific reproductive disorders.

Materials and Methods

Targeting Construct and Generation of Mice. Homologous recombination was used to replace the genomic region of *Brek* that contains 3 exons encoding a part of the kinase domain with the neomycin-resistance (neo) cassette. The DT-A fragment was ligated to the 3′ end of the targeting vector for negative selection. We identified the *Brek*-targeted 129Ola ES cell clones by Southern blot hybridization with the probe shown in Fig. 1*A*, and then injected these cells into C57BL/6 blastocysts. Male chimeras were mated with C57BL/6 females to obtain heterozygous ($Brek^{+/-}$) F1 offspring. We intercrossed the F1 progeny to produce homozygous $Brek^{-/-}$ mice. Genotyping was performed by PCR with specific primers to amplify either the mutant or wild-type allele. All experiments with animals were carried out according to guidelines for animal use issued by the Committee of Animal Experiments, Institute of Medical Science, University of Tokyo.

Histological and TUNEL Analysis. We fixed testes in Bouin's solution or 10% formalin neutral buffer solution. Fixed tissues were embedded in paraffin. Sections (7-μm thick) were cut, dewaxed, and then stained with toluidine blue or by PAS reaction with standard procedures. Apoptotic cells in sections were detected by TUNEL assay with an In Situ Cell Death Detection Kit, Fluorescein (Roche Diagnostics, Tokyo, Japan).

Conventional Transmission Electron Microscopy. We fixed adult testes with 2% glutaraldehyde in 10 mM Hepes buffer. After washing the testes in the same buffer, we cut the tissues into small pieces and immersed them in the same fixative for 2 h at 4°C. Tissues were rinsed with PBS and then fixed again with 2% OsO_4. The samples were dehydrated through graded ethanol series and then embedded in Epon 812. We cut ultrathin sections on an ultramicrotome (Ultracut E; Reichert–Jung, Vienna, Austria) and stained them with uranyl acetate and lead citrate. Staining was observed with a 1200 EX transmission electron microscope (JEOL, Tokyo, Japan).

Immunohistochemical Localization of BREK in the Mouse Testis. Wild type and $Brek^{-/-}$ mice were perfused through the left ventricle with 4% paraformaldehyde in PBS. Testes were removed and immersed in the fixative at 4°C for 4 h. The testis samples were passed through a sucrose gradient (10-, 15-, and 20% in PBS),

and were then incubated in 40% sucrose: optimal cutting temperature (OCT) compound (1:1) overnight at 4°C. The testes were then embedded in OCT compound, frozen in liquid nitrogen, sectioned at 8-μm thickness on a cryostat (model 1720; Lietz, Wetzlar, Germany) and dried for 2 h. After wetting with PBS, the samples were treated with 0.1% Triton X-100 in PBS for 30 min and blocked with 5% normal goat serum and 3% BSA in PBS for 30 min. The samples were then incubated in rabbit polyclonal antibody, KP12 (4 μg/ml; Abcam, Cambridge, U.K.), in PBS at 4°C for 17 h. After washing with PBS, the testis sections were incubated with Alexa Fluor 546 goat anti-rabbit IgG (heavy-chain plus light-chain) (0.8 μg/ml; Molecular Probes, Eugene, OR) and Hoechst 33258 (10 μg/ml; Sigma–Aldrich, St. Louis, MO) for 30 min dissolved in PBS. After washing with PBS, the samples were analyzed with a BX50 microscope (Olympus, Tokyo, Japan) equipped with an imaging system composing of a CCD camera RETIGA Exi FAST 1394 and an imaging soft ware SlideBook 4 (Nippon Roper, Chiba, Japan).

Immunoblot Analysis. Tissue extracts were prepared and analyzed by immunoblotting with antibodies against Brek as described (3).

RT-PCR. Primers were checked by PCR to ensure that they generated single products of the predicted size. Primers for *Prm1*, *Prm2*, *TP1*, *TP2*, *CREM*, and *CaMK4* were kindly provided by A. Urano (University of Tokyo). PCR was performed at typical amplification parameters (95°C for 10 min, followed by 20–30 cycles of 95°C for 30 sec, 55°C for 30 sec, and 72°C for 1 min) by using Ex Taq (TaKaRa Biomedicals, Shiga, Japan) and ABI 9700 thermal cycler (Applied Biosystems, Foster City, CA).

Fractionation of the Normal Testicular Cells. Testes were collected from two male mice (8 weeks of age). The tunica albuginea was removed from each testis. The seminiferous tubules were placed in Eagle's Minimal Essential medium (GIBCO, Carlsbad, CA) containing 0.1% collagenase (Wako Pure Chemical Industries, Osaka, Japan), incubated at room temperature for 1 h with gentle swaying. The tubule suspension was transferred into a conical tube and kept standing for 5 min to precipitate tubule fragments. The supernatant containing separated cells was filtered through a nylon mesh and centrifuged at 600 $\times$ *g* for 10 min. The precipitant was used as a Leydig cell-rich fraction. The remaining tubules were dispersed by gentle pipetting a few times in PBS containing 1 mM EDTA to remove residual Leydig cells. Tubules were then treated with 0.25% Trypsin at 37°C for 10 min, and dispersed by vigorous pipetting. The suspension was filtrated through a nylon mesh and centrifuged at 600 $\times$ *g* for 10 min. The precipitant was dispersed in Eagle's Minimal Essential medium (pH 7.2) containing 10% FBS (GIBCO), transferred to gelatin-coated culture dishes, and incubated at 37°C for 2 h. The culture supernatant was filtered through a nylon mesh and centrifuged at 600 $\times$ *g* for 10 min. The precipitant was used as a germ cell-rich fraction. The cells attached to gelatin-coated culture dishes were washed with PBS a few times and then used as a Sertoli cell-rich fraction.

Assessment of Serum Hormone Levels. The bloods of 8-week-old male *Brek*$^{+/+}$ and *Brek*$^{-/-}$ mice were drawn by cardiocenthesis and incubated at 4°C overnight. After centrifugation at 800 $\times$ *g* for 10 min, the serum was collected and stored at -80°C until analysis. The levels of serum testosterone, luteinizing hormone, and follicle-stimulating hormone were measured by SRL, Tokyo, Japan.

Fertility Assessment. Eight-week-old *Brek*$^{+/-}$ and *Brek*$^{-/-}$ mice were intercrossed. One male was mated with two females for 2 weeks. Female mice were checked for vaginal plugs, and litter sizes were recorded.

Statistical Analysis. Student's *t* test for paired variables was used to examine differences, and data were considered significantly different at $P < 0.05$.

We thank Dr. A. Urano for primers for *Prm1*, *Prm2*, *TP1*, *TP2*, *CREM*, and *CaMK4* and Drs. S. Kina and T. Miyasaka for valuable discussion. This work was supported by grants-in-aid from the Ministry of Education, Culture, Sports, Science, and Technology of Japan.

1. Blume-Jensen P, Jiang G, Hyman R, Lee KF, O'Gorman S, Hunter T (2000) *Nat Genet* 24:157–162.
2. Robinson DR, Wu YM, Lin SF (2000) *Oncogene* 19:5548–5557.
3. Kawa S, Fujimoto J, Tezuka T, Nakazawa T, Yamamoto T (2004) *Genes Cells* 9:219–232.
4. Wang H, Brautigan DL (2002) *J Biol Chem* 277:49605–49612.
5. Kesavapany S, Lau KF, Ackerley S, Banner SJ, Shemilt SJ, Cooper JD, Leigh PN, Shaw CE, McLoughlin DM, Miller CC (2003) *J Neurosci* 23:4975–4983.
6. Reith AD, Rottapel R, Giddens E, Brady C, Forrester L, Bernstein A (1990) *Genes Dev* 4:390–400.
7. Meistrich ML (1977) *Methods Cell Biol* 15:15–54.
8. Gaozza E, Baker SJ, Vora RK, Reddy EP (1997) *Oncogene* 15:3127–3135.
9. Tomomura M, Hasegawa Y, Hashikawa T, Tomomura A, Yuzaki M, Furuichi T, Yano R (2003) *Brain Res Mol Brain Res* 112:103–112.
10. Raghunath M, Patti R, Bannerman P, Lee CM, Baker S, Sutton LN, Phillips PC, Damodar Reddy C (2000) *Brain Res Mol Brain Res* 77:151–162.
11. Tomomura M, Fernandez-Gonzales A, Yano R, Yuzaki M (2001) *Oncogene* 20:1022–1032.
12. Tomomura M, Furuichi T (2005) *J Biol Chem* 280:35157–35163.
13. Parvinen M, Pelto-Huikko M, Soder O, Schultz R, Kaipia A, Mali P, Toppari J, Hakovirta H, LonnerbSmeyne RJ, Klein R, *et al.* (1994) *Nature* 368:246–249.
14. Barbacid M (1994) *J Neurobiol* 25:1386–1403.
15. Nakamura T, Yao R, Ogawa T, Suzuki T, Ito C, Tsunekawa N, Inoue K, Ajima R, Miyasaka T, Yoshida Y, *et al.* (2004) *Nat Genet* 36:528–533.
16. Urano A, Endoh M, Wada T, Morikawa Y, Itoh M, Kataoka Y, Taki T, Akazawa H, Nakajima H, Komuro I, *et al.* (2005) *Mol Cell Biol* 25:6834–6845.
17. Weissenberg R, Eshkol A, Lunenfeld B (1982) *Arch Androl* 9:135–140.
18. Varmuza S, Jurisicova A, Okano K, Hudson J, Boekelheide K, Shipp EB (1999) *Dev Biol* 205:98–110.
19. Alessi D, MacDougall LK, Sola MM, Ikebe M, Cohen P (1992) *Eur J Biochem* 210:1023–1035.
20. Park C, Choi WS, Kwon H, Kwon YK (2001) *Mol Cells* 12:360–367.
21. Li C, Watanabe G, Weng Q, Jin W, Furuta C, Suzuki AK, Kawaguchi M, Taya K (2005) *Zoolog Sci* 22:933–937.
22. Feng C, Zhang J, Gasana V, Fu W, Liu Y, Zong Z, Yu B (2005) *Cell Biochem Funct* 23:415–420.
23. Huynh T, Mollard R, Trounson A (2002) *Hum Reprod Update* 8:183–198.
24. Fitch N, Richer CL, Pinsky L, Kahn A (1985) *Am J Med Genet* 20:31–42.